ACS Infectious Diseases

Article

pubs.acs.org/journal/aidcbc

Fluorescent Trimethoprim Conjugate Probes To Assess Drug Accumulation in Wild Type and Mutant *Escherichia coli*

Wanida Phetsang, Ruby Pelingon, Mark S. Butler, Sanjaya KC, Miranda E. Pitt, Geraldine Kaeslin, Matthew A. Cooper,* and Mark A. T. Blaskovich*

Institute for Molecular Bioscience, The University of Queensland, Brisbane, Queensland 4072, Australia

Supporting Information

ABSTRACT: Reduced susceptibility to antimicrobials in Gram-negative bacteria may result from multiple resistance mechanisms, including increased efflux pump activity or reduced porin protein expression. Up-regulation of the efflux pump system is closely associated with multidrug resistance (MDR). To help investigate the role of efflux pumps on compound accumulation, a fluorescence-based assay was developed using fluorescent derivatives of trimethoprim (TMP), a broad-spectrum synthetic antibiotic that inhibits an intracellular target, dihydrofolate reductase (DHFR). Novel fluorescent TMP probes inhibited *e*DHFR activity with comparable potency to TMP, but did not kill or inhibit growth of wild type *Escherichia coli*. However, bactericidal activity was observed against an efflux pump deficient *E. coli* mutant strain (Δ*tolC*). A simple and quick fluorescence assay was developed to measure cellular accumulation of the TMP probe using either fluorescence spectroscopy or flow cytometry, with validation by LC-MS/MS. This fluorescence assay may provide a simple method to assess efflux pump activity with standard laboratory equipment.

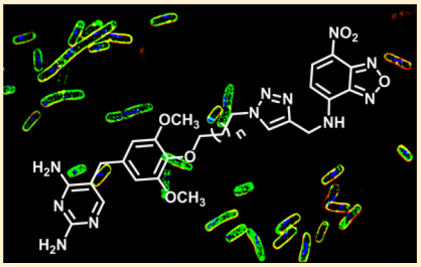

KEYWORDS: *antibiotics, efflux pump, fluorescent probes, cellular accumulation, trimethoprim*

The rise of multidrug-resistant (MDR) bacteria is causing significant healthcare issues.[1] These MDR bacteria typically employ a combination of four main strategies to combat antibiotics: (i) prevention of intracellular antibiotic accumulation via efflux pumps and decreased outer membrane permeability; (ii) target modification; (iii) antibiotic inactivation; and (iv) acquisition of alternate metabolic pathways.[2,3] Gram-negative bacteria are usually less susceptible to antibiotics compared to Gram-positive bacteria due to their dual membrane structure, combined with facile up-regulation of efflux pumps so that intracellular antibiotic concentrations do not reach cytotoxic concentrations.[4,5] The lack of activity of many narrow-spectrum Gram-positive selective antibiotics against Gram-negative bacteria is often caused by efflux mechanisms.[6] For example, it has been shown that Gram-negative bacteria become susceptible to linezolid, clarithromycin, and erythromycin[7] when specific efflux pump genes have been deleted.[8] In particular, the efflux effect has implications for the design of new antibiotic drugs,[9] as potentially unique antibiotic structures or those acting on novel targets may be discarded on the basis of poor activity in minimum inhibitory concentration (MIC) assays resulting from high efflux. It may be possible to develop these as new antibiotics if co-administered with an efflux pump inhibitor or to optimize their structure to remove efflux pump susceptibility and increase their ability to diffuse through porin channels.[10] Improving our understanding of how whole cell activity correlates with in vitro enzyme inhibition requires assessment of the intracellular accumulation of antibiotics and the role of efflux pumps.

Bacterial efflux pumps are membrane transporter proteins that facilitate the uptake and excretion of compounds[11,12] and play important roles in cell-to-cell communication, bacterial pathogenicity, and biofilm formation.[12,13] There are four main protein families for efflux pump systems: ATP-binding cassette superfamily (ABC) proteins, the major facilitator superfamily (MFS) transport proteins, small multidrug resistance (SMR) transporters, and multidrug and toxic compound extrusion (MATE) proteins, which are all present in both Gram-positive and Gram-negative bacteria. A fifth family, the resistance nodulation cell division (RND) pump, is found only in Gram-negative bacteria. Efflux pumps can contain multiple components, with an inner membrane transporter, a periplasmic adaptor protein, and an outer membrane channel that together are able to directly extrude various drugs from inside to outside the cell.[4,8,13,14] Some efflux pumps are specific for particular substrates, whereas other efflux pumps can transport a wide range of substrates with various chemical structures. Up-regulation of efflux pumps contributes to the development of MDR bacteria.[10,14]

Fluorescent probes are versatile tools for biological study imaging, with different color combinations used to investigate specific target sites and to show biological events in living cells.[15] For example, antibiotic fluorescent probes have been used to investigate cell division in Gram-positive bacteria.[16−20] Detection of fluorescence can be used for both quantitative and

Received: May 16, 2016
Published: August 5, 2016

DOI: 10.1021/acsinfecdis.6b00080
ACS Infect. Dis. 2016, 2, 688−701

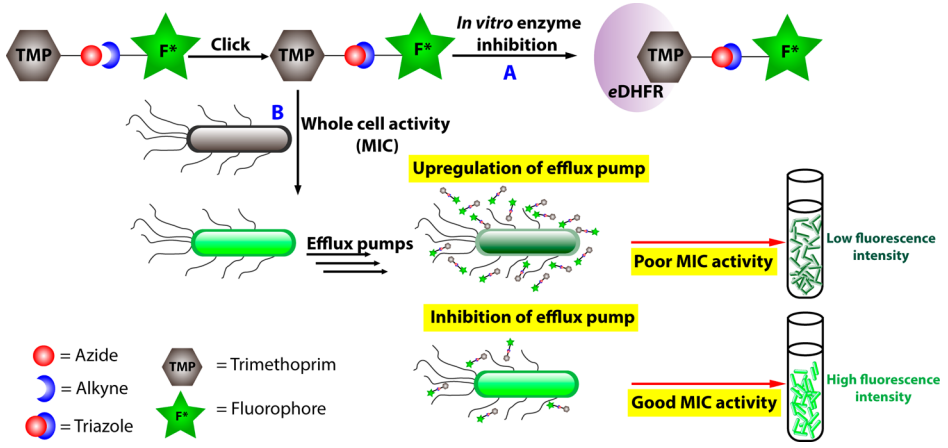

Figure 1. Use of fluorescently labeled antibiotics to assess efflux in Gram-negative bacteria without cell lysis: (A) in vitro enzyme inhibition (IC_{50}), enzyme binding and inhibition by fluorescent antibiotic; (B) whole cell activity (MIC), fluorescent probe loses MIC activity due to efflux pumps. Fluorescence intensity can quantify the efflux effect.

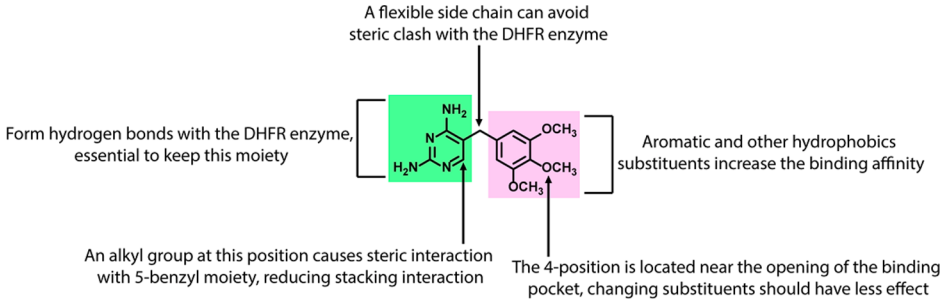

Figure 2. Known structure−activity relationships of trimethoprim.

qualitative analysis[21] of the labeled cell,[22] bacteria,[23] or nanoparticles[24] and also to detect bacterial infections in vivo.[25]

We have initiated a program to develop fluorescent probes based on all major classes of antibiotics. To prepare antibiotic-derived fluorescent probes, it is necessary to identify a suitable position on the antibiotic to link with the fluorophore so that the new derivative maintains antimicrobial activity. Published structure−activity relationship (SAR) studies can pinpoint sites that are able to tolerate structural changes. As antibiotics often possess multiple functional groups with various reactivities, we need to employ an orthogonal reaction that is compatible with various functional groups to systematically prepare fluorescent antibiotics of all major antibiotic classes. One such reaction is the Cu-catalyzed azide−alkyne cycloaddition (CuAAC) reaction that forms a stable and biocompatible triazole ring in the presence of unprotected functional groups (such as amines, hydroxyls, and thiols) or reactive moieties (such as lactams, epoxides, or α,β-unsaturated systems).[26] The precursor azide and alkyne groups are known for their biocompatibility and selective reactivity as bio-orthogonal chemical reporters. For example, azides have been installed in the outer membrane (OM) of bacteria and also embedded within glycans. The resulting azido residues were labeled with various probes via cycloaddition with alkynes using either copper(I)-mediated or strain-promoted [3+2] cycloadditions.[27,28] Meanwhile, terminal alkyne and cyclooctyne substituents have been widely used to link with dyes/markers or nanoparticles for therapeutic and diagnostic applications.[29−31] In this study, the azide functionality was selected for antibiotic modification, given the more facile introduction of an azide group to highly diverse antibiotic cores compared to an alkyne. These azide-functionalized antibiotics also have potential for the development of diagnostics or sensing applications.[32]

We recently described an oxazolidinone-derived (linezolid) azide-functionalized antibiotic intermediate that was conjugated with fluorophores, with the resulting probes then used to image Gram-positive bacteria.[33] This same strategy has now been employed to prepare TMP fluorescent derivatives. TMP is a synthetic antibiotic that acts on an intracellular bacterial target, dihydrofolate reductase (DHFR). In clinical use, it is normally administered in combination with sulfamethoxazole (SMZ), which inhibits another step in the folic acid pathway. The TMP−SMZ combination is used to treat a wide range of infections caused by Gram-negative bacteria (such as the Enterobacteriaceae family and *Haemophilus influenza*) and Gram-positive bacteria (such as *Staphylococcus aureus* and *Streptococcus pneumoniae*).[34,35] TMP fluorescent probes have previously been applied to a general strategy for labeling targets in mammalian cell live cell imaging; the protein of interest was tagged with *Escherichia coli* DHFR (*e*DHFR) and then labeled with a cell-permeable TMP probe.[36−43] Nevertheless, there have been no reports of applying TMP fluorescent probes to bacterial cells.

We also describe the development of a simple fluorescence-based assay using flow cytometry or fluorescence spectroscopy to assess efflux pump activity that affects the accumulation of fluorescent-labeled TMP in *E. coli* (Figure 1). The fluorescence-based assay was validated by liquid chromatography−mass spectrometry (LC-MS/MS) quantification that measured probe cellular concentrations. These methods that can measure the

DOI: 10.1021/acsinfecdis.6b00080
ACS Infect. Dis. 2016, 2, 688−701

cellular concentration of the fluorescent probes could potentially be used to screen for efflux inhibitors, assess up-regulation of efflux in antibiotic-resistant bacteria, and assist in new antibiotic development.

RESULTS AND DISCUSSION

Design and Synthesis of TMP-Linked Fluorophores. On the basis of published SAR of TMP derivatives and fluorescent TMP probes that have previously been prepared,[44] we proposed that modification at position 4 of the TMP phenyl ring was possible without sacrificing significant activity (Figure 2).[41,45,46] As antibiotics and fluorophores often possess reactive moieties and multiple functional groups with varied reactivity, an orthogonal reaction compatible with reactive moieties and many different functional groups was required. TMP has unprotected amines that can act as nucleophiles (reactive for alkylation and amide condensation reactions).[47] Moreover, fluorophores such as coumarin-based fluorophores and rhodamine derivatives contain heterocyclic rings, which are sensitive to ring opening.[48] In line with our overall goal of producing a "toolset" of azide-functionalized antibiotics that can be readily linked with different colored fluorophores, we selected the CuAAC reaction for antibiotic−probe conjugation. Low molecular weight fluorophores are more suitable for retaining antimicrobial activity as large highly hydrophobic fluorophores are likely to aggregate and have difficulty in penetrating through the bacterial membrane, as well as potentially disrupting DHFR target binding. Therefore, three comparatively small fluorophores, 7-(dimethylamino)-coumarin-4-acetic acid (DMACA), 7-nitrobenzofurazan (NBD), and dansyl (DNS, dimethylaminosulfonyl) (Figure 3), were each functionalized with an alkyne substituent for CuAAC reactions with the azide-substituted TMP derivatives.

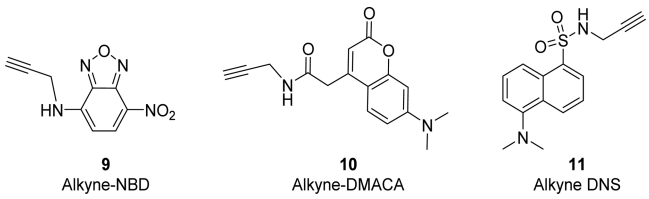

Figure 3. Alkyne-derivatized fluorophores.

The synthesis of the TMP analogues was based on a mild and efficient procedure reported by Ji et al. in 2013.[49] In short, TMP derivatives **8** were synthesized from syringaldehyde **1** by alkylation with bromo−chloro alkane linkers in the presence of K_2CO_3 in DMF at 60 °C (Scheme 1). Treatment of **3** with sodium azide at 100 °C in the presence of sodium iodide gave azidobenzaldehyde **4**. Aldol condensation and 1,3-prototropic isomerization between azidobenzaldehyde **4** and 3-morpholinopropionitrile in the presence of the catalytic amount of potassium hydroxide and methanol provided the intermediate **6**, which was followed by in situ acid-mediated substitution of the 3-dimethylamino group with aniline with a convenient one-pot procedure that resulted in enamine **7**. Cyclization of the enamine **7** with guanidine provided azide-TMPs **8a−c** in high yield.

The alkyne derivatives **9** and **10** (Figure 3) of fluorophores NBD and DMACA were prepared according to literature procedures,[33] whereas the DNS-alkyne **11** was synthesized via sulfonamide coupling of dansyl chloride and propargylamine in the presence of triethylamine.

TMP-azide derivatives **8a−c** underwent CuAAC reaction with the alkyne-fluorophores **9−11** in the presence of sodium ascorbate and copper sulfate to produce probes **12−14a−c**. At room temperature or even with heating at 50 °C, reactions often took days to produce the desired products despite the putative facile nature of the CuAAC reaction, so microwave heating at 100 °C was applied to accelerate the reaction rates (Scheme 2).

Biological Activity. The TMP derivatives **8a−c** were tested for their ability to inhibit *e*DHFR and their antimicrobial activities assessed against wild type and mutant *E. coli* strains (Table 1). The azide-TMPs retained moderate antimicrobial activity, with the shortest linker **8a** showing the best activity, although still 8−16-fold less active than TMP itself. Unfortunately, all of the TMP fluorescent probes lost antimicrobial activity (>64 μg/mL), even though they were still able to inhibit *e*DHFR with comparable, or only 2−5-fold reduced, potency, relative to TMP. The ability to inhibit eDHFR tended to decrease with longer linker length for both azides and probes. These results suggested the loss of activity of TMP derivatives was due to an inability to access the DHFR target within the bacterial cell.

Interestingly, the antimicrobial activities of the TMP probe were restored against an *E. coli* Δ*tolC* mutant, lacking the TolC efflux pump component, with the probes **12−14a−c** (0.25−8 μg/mL) showing potency almost as good as TMP (0.125 μg/mL) (Table 1). These MIC results indicated that the lack of whole cell activity was likely due to compound efflux. In addition, the TMP probes were tested against membrane-impaired mutant *E. coli* (LpxC and DC2), which are more permeable to many compounds. Somewhat unexpectedly, the antimicrobial activity of the TMP probes were not improved (TMP; MIC = 0.25−0.5, **12−14a−c**; MIC > 64 μg/mL), implying that the ability to penetrate into the cells was not limiting their effectiveness. Although these two permeable membrane mutants provide general membrane disruption, they do not affect the porin channels, outer membrane proteins (OMPs) that largely control influx, so the ability of the TMP probes to penetrate by diffusion via porin channels has not been assessed. Porin penetration by the TMP probes would be expected to be affected by the increase in size caused by attachment of the fluorophore (e.g., **12b** = 592 Da compared to TMP, 290 Da).

For the set of probes prepared, antimicrobial activity tended to improve for all fluorophore conjugates with a longer linker, whereas for a fixed linker the DMACA fluorophore was consistently the least active of the three fluorophores. DNS possessed the best activity for C3 (n = 1) and C5 (n = 3) linker lengths, but NBD the best for C4 (n = 2). Activity against mutant *E. coli* possessing both *lpxC* and *tolC* mutations was comparable to the single mutant *E. coli tolC*, confirming that the TolC-dependent efflux pumps were most responsible for the poor MIC activity.

The TMP probes were not generally cytotoxic against mammalian kidney and liver cell lines at the highest concentration tested (CC_{50} > 60 μM). Therefore, these probes could also find utility for live cell fluorescence imaging studies in mammalian cell lines, for example, studying ATP-binding cassette superfamily (ABC) efflux pumps in cancer cells that are responsible for extruding chemotherapeutic agents, leading to the reduction of intracellular drug level and resistance.[50]

DOI: 10.1021/acsinfecdis.6b00080
ACS Infect. Dis. 2016, 2, 688−701

Scheme 1. Synthesis of Trimethoprim-Linked Azides 8a−c

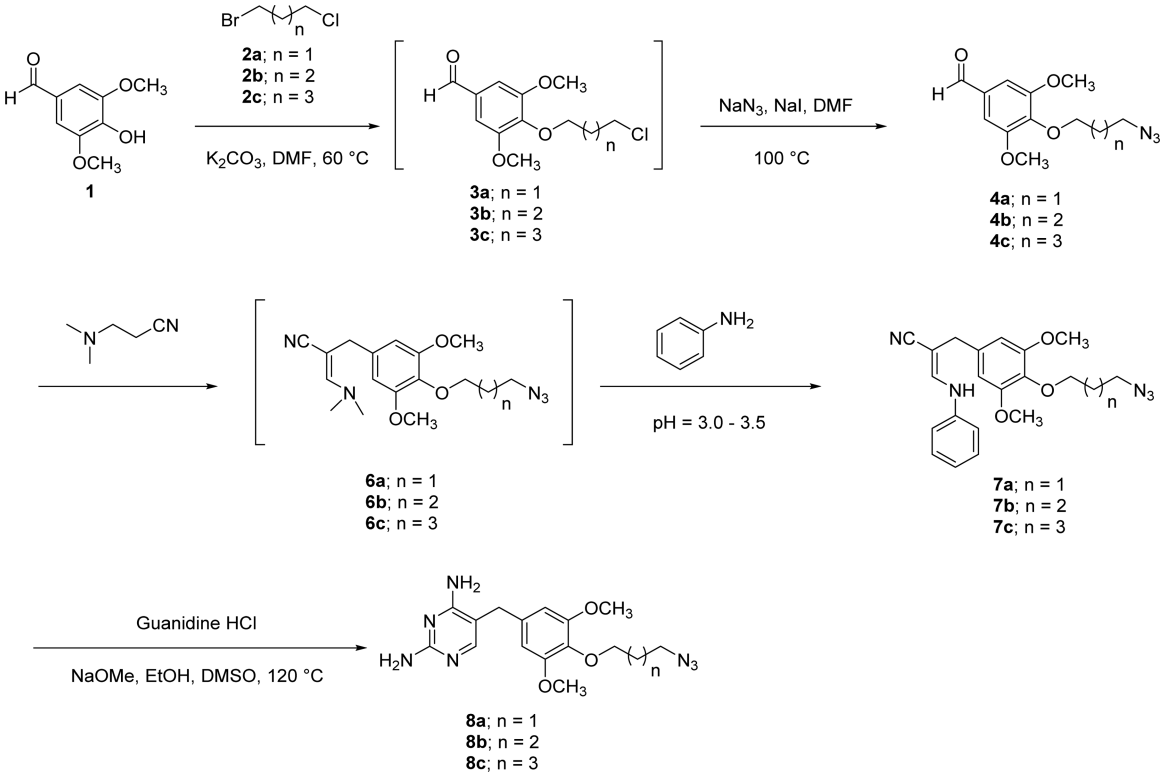

Scheme 2. Synthesis of Trimethoprim Probes Using Microwave-Assisted Click Chemistry

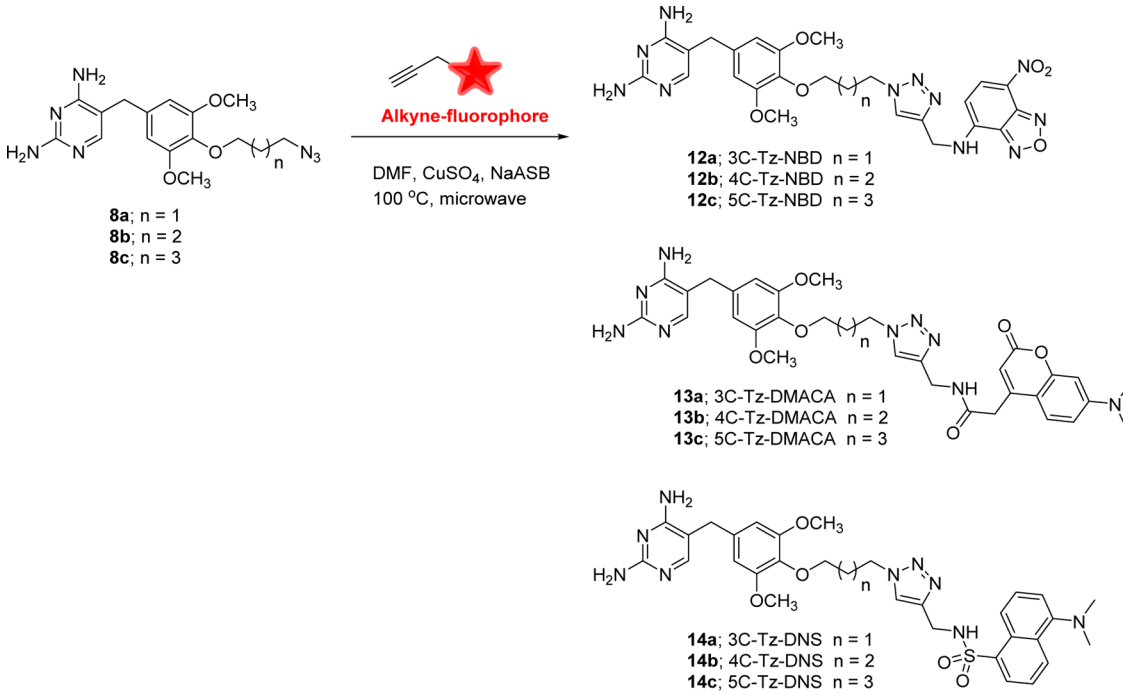

Use of the Fluorescent TMP Probe To Measure Efflux Pump Activity. Complete sequencing of bacterial genomes has revealed that *E. coli* contains at least 37 efflux pump transporters including 7 ABC, 19 MFS, 1 MATE, 5 SMR, and 7 RND.[51] The source of energy utilized by MFS, SMR, and RND pumps is the proton motive force (PMF), whereas the ABC transporter obtains energy from ATP hydrolysis and the MATE pumps use a Na^+ gradient as a driving force.[52] However, the AcrAB-TolC system, which belongs to the tripartite RND family, is considered to be the predominant pump in *E. coli* for multidrug resistance.[12] To further investigate the effects of the TolC-dependent efflux pump system and other efflux pumps influencing the susceptibility of *E. coli* to the TMP probes, we developed a fluorescence assay to measure cellular accumulation of the TMP probes in *E. coli* in the presence and absence of carbonyl cyanide *m*-chlorophenylhydrazone (CCCP). CCCP

DOI: 10.1021/acsinfecdis.6b00080
ACS Infect. Dis. 2016, 2, 688−701

Table 1. MIC Activities of TMP Probes against *E. coli* and Inhibition of *e*DHFR Enzyme (n = 4)[a]

compound		MIC (μg/mL)									cytotoxicity (CC_{50}) (μM)		*e*DHFR inhibition IC_{50} (nM)
		E. coli ATCC 25922	*E. coli* clin isol	*E. coli* clin isol	*E. coli* MB4827	*E. coli* DC2 mutant	*E. coli* *lpxC* mutant	*E. coli* *tolC* mutant	*E. coli* *lpxC/tolC* mutant	*S. aureus* ATCC 25923	HEK 293	HepG2	
TMP		0.5	0.5	0.5	1	**0.25**	**0.5**	**0.125**	**0.125**	1	>60	>60	60
8a	TMP-3C-N_3	8	8	4	8	**4**	**8**	**0.25**	**0.25**	4	>60	>60	66
12a	TMP-3C-Tz-NBD	>64	>64	>64	>64	**>64**	**>64**	**2**	**1**	64	>60	>60	254
13a	TMP-3C-Tz-DMACA	>64	>64	>64	>64	**>64**	**>64**	**8**	**8**	>64	>60	>60	83
14a	TMP-3C-Tz-DNS	>64	>64	>64	>64	**>64**	**>64**	**0.5**	**0.5**	>64	59	>60	162
8b	TMP-4C-N_3	32	8	16	16	**8**	**8**	**0.125**	**0.25**	4	>60	>60	97
12b	TMP-4C-Tz-NBD	>64	>64	>64	>64	**>64**	**>64**	**0.25**	**0.5**	16	>60	>60	148
13b	TMP-4C-Tz-DMACA	>64	>64	>64	>64	**>64**	**>64**	**2**	**2**	>64	>60	>60	162
14b	TMP-4C-Tz-DNS	>64	>64	>64	>64	**>64**	**>64**	**0.5**	**1**	64	59	>60	226
8c	TMP-5C-N_3	32	16	16	32	**8**	**8**	**0.125**	**0.25**	4	>60	>60	140
12c	TMP-5C-Tz-NBD	>64	>64	>64	>64	**>64**	**>64**	**0.5**	**0.5**	8	46	>60	208
13c	TMP-5C-Tz-DMACA	>64	>64	>64	>64	**>64**	**>64**	**1**	**1**	>64	>60	>60	668
14c	TMP-5C-Tz-DNS	>64	>64	>64	>64	**>64**	**>64**	**0.25**	**0.25**	32	32	51	509

[a]Clin isol, clinical isolate; wild type HEK 293, human embryonic kidney 293; HepG2, liver hepatocellular cells.

DOI: 10.1021/acsinfecdis.6b00080
ACS Infect. Dis. 2016, 2, 688−701

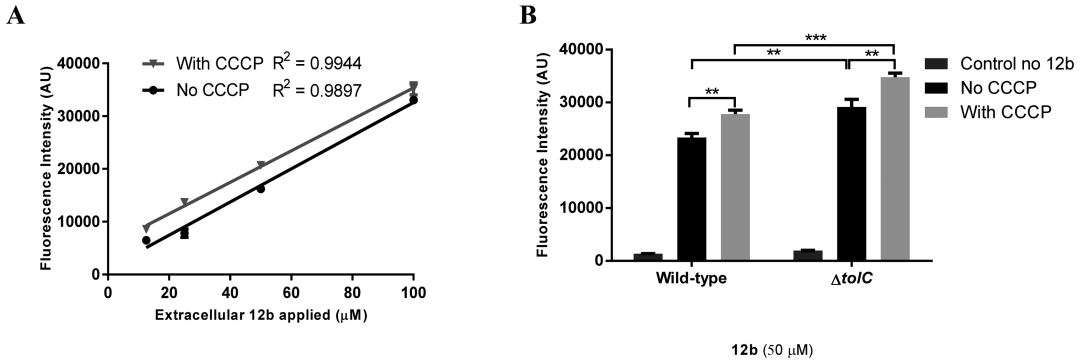

Figure 4. Fluorescence spectroscopic measurement of cellular accumulation of **12b** in *E. coli*. (A) Fluorescence intensity in *E. coli* (ATCC 25922) incubated with **12b** at various concentrations with/without pretreatment with CCCP (100 μM at 37 °C for 10 min). Statistical significance was assessed using a linear regression of fluorescence intensity against concentration and experimental groups. The model was refitted without an interaction term, giving an estimated fluorescence intensity difference between the groups of 3622.250, with p value 2.52×10^{8}, ***. (B) Fluorescence intensity in *E. coli* (Δ*tolC*) and *E. coli* (ATCC 25922) incubated with **12b** at 50 μM with/without pretreatment with CCCP (100 μM at 37 °C for 10 min). Statistical significance (**, $p \leq 0.01$; ***, $p \leq 0.001$) is shown between the absence or presence of CCCP and between wild type and Δ*tolC E. coli*. Data reported are the mean ± SD for three experiments.

collapses the PMF energizing most *E. coli* efflux pumps,[53] thus inactivating them, and has been used to study cellular accumulation in Gram-negative bacteria for a wide range of compounds.[11,54,55]

The most potent TMP probe, **12b** (*E. coli* wild type MIC > 64 μg/mL, *E. coli* mutant deficient *tolC* MIC = 0.25 μg/mL, *e*DHFR IC_{50} = 148 nM), was selected to develop a fluorescent bacterial accumulation assay. Two strains of *E. coli* were tested: wild type (ATCC 25922) and mutant *E. coli* (Δ*tolC*). Various cell densities from wild type *E. coli* were evaluated to assess the number of bacteria required for significant fluorescence intensity: densities of OD_{600} = 2 were required to provide sufficient signal when 1 mL of bacteria was centrifuged, resuspended in 150 μL of PBS, and measured in a 96-well plate on a Tecan plate reader at 475 nm excitation/545 nm emission.

To assess the effect of efflux pump inhibition, *E. coli* was pretreated with CCCP (100 μM) for 10 min before incubation with **12b**. Under this condition, the fluorescence intensity of CCCP-treated wild type *E. coli* significantly increased compared to untreated *E. coli* (Figure 4A), confirming that accumulation of **12b** increased when efflux pump systems were inhibited. The concentration dependence of compound accumulation was investigated by treating *E. coli* with concentrations of **12b** ranging from 12.5 to 100 μM. Interestingly, a linear increase of cellular accumulation of **12b** was observed, indicating a concentration-dependent cellular accumulation. Accumulation of **12b** in the untreated *E. coli* also increased linearly even though the efflux pump systems were functional and capable of exporting the probe **12b** to the outside of the bacterial cells. This linearity is consistent with a literature paper that showed a dose-dependent accumulation of sulfonyladenosine between 10 and 1000 μM in *E. coli* (ATCC 25922).[54] Another study, examining accumulation of ciprofloxacin in wild type *Pseudomonas aeruginosa*, also showed an apparent linear accumulation, with a 4-fold cellular increase when the bacteria were treated with ciprofloxacin at 100 ng/mL compared to ciprofloxacin at 25 ng/mL.[55]

In Gram-negative bacteria, most OMPs are porins, water-filled open channels that allow passive diffusion of small hydrophilic molecules up to 600 Da across the OM. These porin channels are driven by a concentration gradient. Thus, the kinetics of uptake largely depend on the concentration gradient of the solute. With the size of **12b** (592 Da) and its hydrophilicity, **12b** may traverse the bacterial cell wall through porins, providing the observed linear concentration-dependent cellular accumulation.[4,56,57] Although efflux pumps were functional in the untreated (no CCCP) wild type *E. coli* group, the overall accumulation depends on the relative rates of influx rate via porins versus efflux rate via efflux pumps. It is important to highlight that because porins discriminate solutes on the basis of the physicochemical properties of compounds, the size of potential fluorescent antibiotic conjugates for fluorescence assays must be considered; if they are too large to diffuse into bacterial cells via porins, they would be ineffective as probes of efflux pump activity.

A similar study was conducted with the TolC-deficient (Δ*tolC*) strain, but because **12b** was much more active against this strain (MIC = 0.25 μg/mL = 0.37 μM), a maximum concentration of 50 μM **12b** was employed (Figure 4B). Notably, CCCP-treated Δ*tolC E. coli* also showed higher fluorescence intensity compared to untreated Δ*tolC E. coli*. This result indicates that, in the Δ*tolC* strain, other TolC-independent efflux pumps that obtain energy from the PMF are exporting **12b**.

As expected from the variation in antibiotic susceptibility, accumulation of **12b** in wild type *E. coli* was significantly less than in Δ*tolC E. coli* when bacteria were incubated with the same concentration of **12b** at 50 μM. This result showed the effect of TolC at reducing the cellular accumulation of **12b**. The AcrAB-TolC efflux system, known as the predominant pump in multidrug-resistant *E. coli*, is composed of an inner membrane transporter, a periplasmic adaptor protein, and outer membrane channel (TolC), so this tripartite system becomes nonfunctional when any of these components is absent.[58,59]

Flow Cytometric Analysis. Flow cytometry can be used to assess bacterial characteristics related to size and intrinsic and extrinsic fluorescence in cells. Quantitative measurement of the staining intensity of probes in bacteria has been used for different purposes such as discrimination between Gram-positive and Gram-negative strains, bacteria viability, and antibiotic susceptibility testing.[60−62] Recently, flow cytometry analysis was used to measure cellular fluorescence in *B. subtilis* to quantitatively evaluate labeling levels of amino acids on the cell surface.[63] To investigate whether flow cytometric analysis

DOI: 10.1021/acsinfecdis.6b00080
ACS Infect. Dis. 2016, 2, 688−701

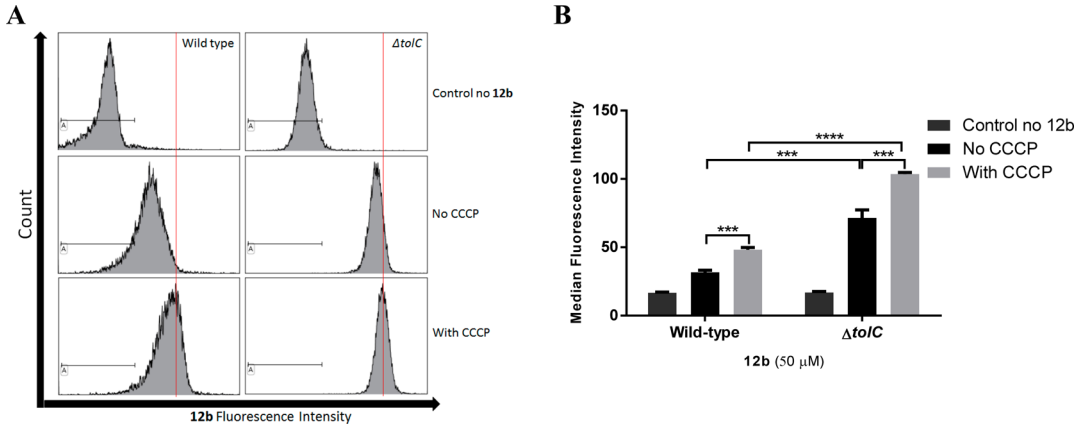

Figure 5. Flow cytometry measurement of cellular accumulation of **12b** at 50 μM in *E. coli* (ATCC 25922) and *E. coli* (Δ*tolC*) with/without pretreatment with CCCP (100 μM at 37 °C for 10 min). (A) Histograms of **12b**. Red line shows shift of fluorescence intensity. (B) Median fluorescence intensity of **12b**. The data were collected from 10000 bacterial events. Statistical significance (***, $p \leq 0.001$; ****, $p \leq 0.0001$) is shown between the absence and presence of CCCP and between wild type and Δ*tolC E. coli*. Data reported are the mean ± SD for three experiments.

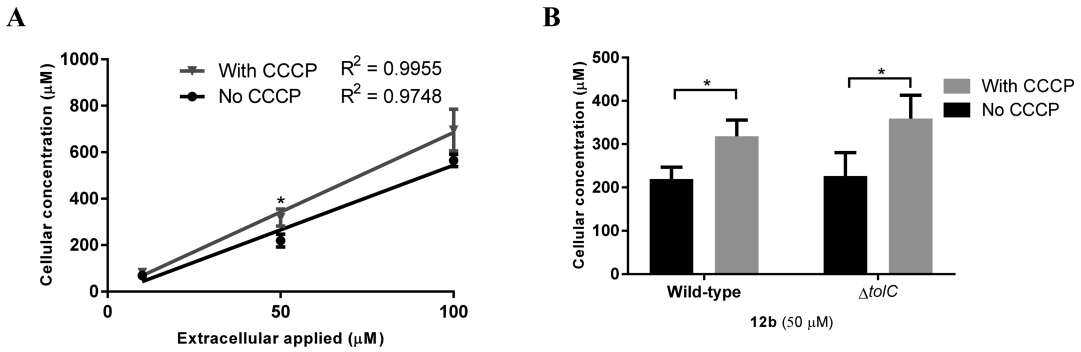

Figure 6. LC-MS measurement of accumulation of TMP derivative **12b** in *E. coli*. (A) *E. coli* (ATCC 25922) was incubated with **12b** at vaious concentrations with/without pretreatment with CCCP (100 μM at 37 °C for 10 min). (B) *E. coli* (Δ*tolC*) and *E. coli* (ATCC 25922) were incubated with **12b** at 50 μM with/without pretreatment in the presence and absence of CCCP (100 μM at 37 °C for 10 min). A significant difference (*, $p \leq 0.05$) was shown between the absence and presence of CCCP. The cellular concentration was calculated from the lysate concentration of 2×10^9 bacteria cells. Data reported are the mean ± SD for three experiments.

could be used to measure cellular accumulation of fluorescent TMP, bacteria samples were prepared and treated with **12b** (50 μM) in the same way as the fluorescence spectroscopy-based assay. Bacteria pellets were resuspended in 1 mL of PBS, with their fluorescence intensity measured using the flow cytometer. Variations in the fluorescence intensity led to shifts in the histogram peaks (Figure 5A), with measurement of the mean fluorescence intensity of the histograms providing a quantitative analysis.

Flow cytometry showed that the fluorescence intensity of **12b** in both CCCP-treated wild type and Δ*tolC E. coli* was greater than when the efflux pumps were not inhibited and that the Δ*tolC E. coli* intensity was greater than that of wild type *E. coli*. This result matched those provided by the fluorescence spectroscopy-based assay, although with more distinct differences between the groups (Figure 5B). Thus, either method can be used to assess cellular accumulation of fluorescent-labeled antibiotics.

LC-MS/MS-Based Bacterial Accumulation Assay. We wished to confirm that the fluorescence measurements correlated with the cellular concentration of the TMP probes. LC-MS/MS is an accurate quantification method that has previously been reported as a general method to measure compound accumulation within cells.[54,55] Although it does not allow for visualization of compound distribution within a cell and is too time-consuming for rapid screening, the LC-MS/MS method does allow for direct measurement of unaltered parent compound, which is an advantage over the labeled probe methods requiring compound modifications. After probe treatment, the bacteria were first washed to remove any surface-bound compound and then lysed to release compound accumulated within the cell. Previous studies have applied sonication, mechanical cell lysis, and/or overnight incubation with glycine−HCl (pH ≤3) to lyse bacteria;[54,55,64] however, these lysis procedures are time-consuming and not suitable for high-throughput analyses. Therefore, we used lysozyme, a muramidase that is able to lyse both Gram-positive and Gram-negative bacteria[65,66] by cleaving bacterial peptidoglycan between the glycosidic β-1,4-linked *N*-acetylmuramic acid (MurNAc) and *N*-acetylglucosamine (GlucNAc).[67] The lysozyme lysis buffer usually consists of Tris-HCl (pH 8), EDTA, and a detergent such as Triton X-100, but to improve our LC-MS analysis detection sensitivity, the detergent component was removed to avoid MS ion suppression and decreased HPLC resolution.[68] Because the detergent component was required for disruption of the cell membrane, sonication and freeze−thaw steps were added to ensure that the bacterial cells were broken.

DOI: 10.1021/acsinfecdis.6b00080
ACS Infect. Dis. 2016, 2, 688−701

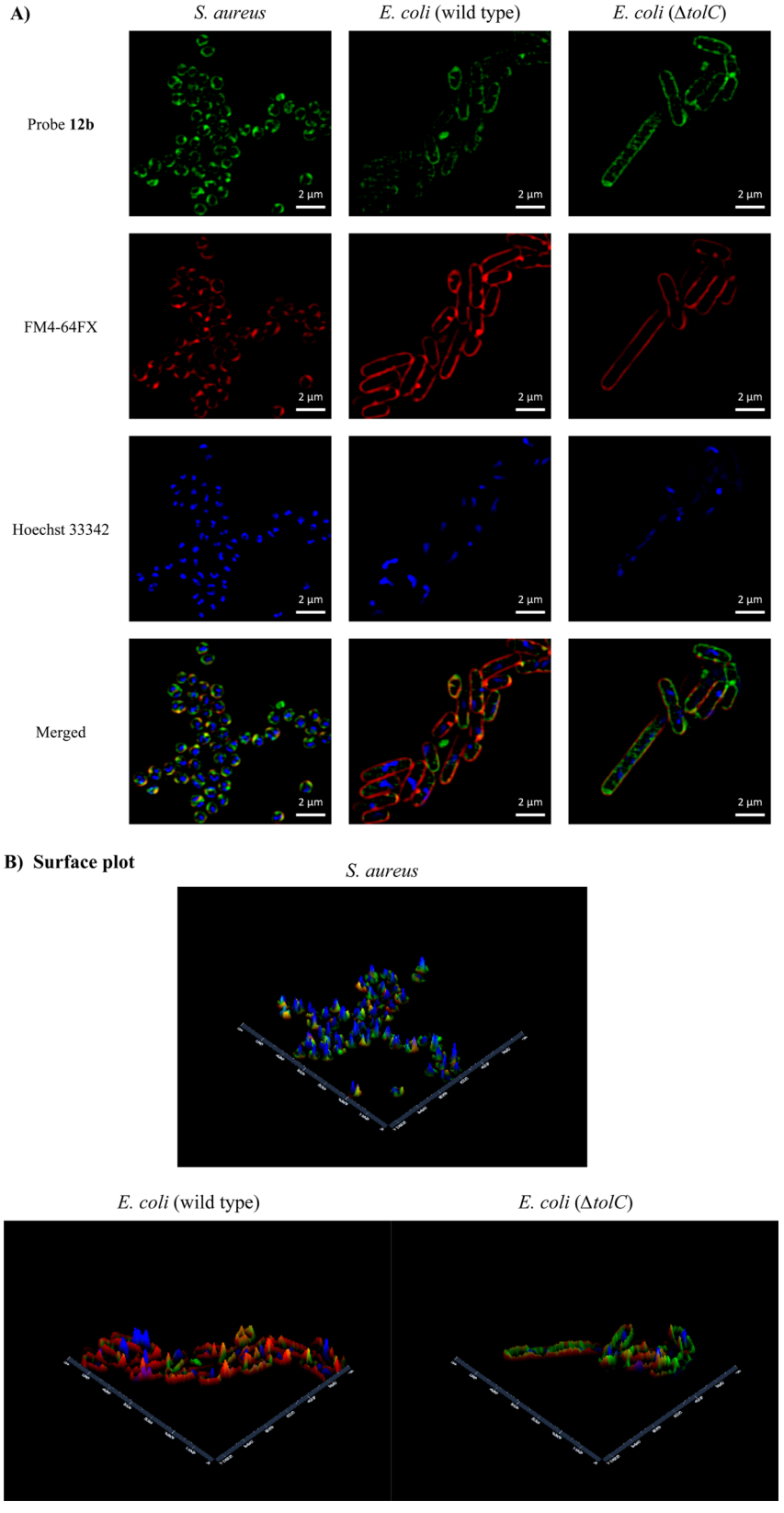

Figure 7. (A) SR-SIM fluorescence imaging of *S. aureus* (ATCC 25923) and *E. coli* (ATCC 25922 and Δ*tolC*): green, TMP-fluorophore **12b**; red, FM4-64FX (bacterial membrane stain); blue, Hoechst 33342 (nucleic acid stain). (B) Surface plot: *X*, *Y* axes indicate distance (nm). The scale bar shown represents 2 μm.

Following cell lysis, lysozyme (14.3 kDa) was removed using a filter membrane (10 kDa). The filtrate containing cell lysate (molecular mass < 10 kDa) and any cellular-localized probe were collected, lyophilized, and redissolved in the solution mixture containing **12a** as an internal standard. Probe **12a** was used as an internal standard as it has a structure similar to that

DOI: 10.1021/acsinfecdis.6b00080
ACS Infect. Dis. 2016, 2, 688−701

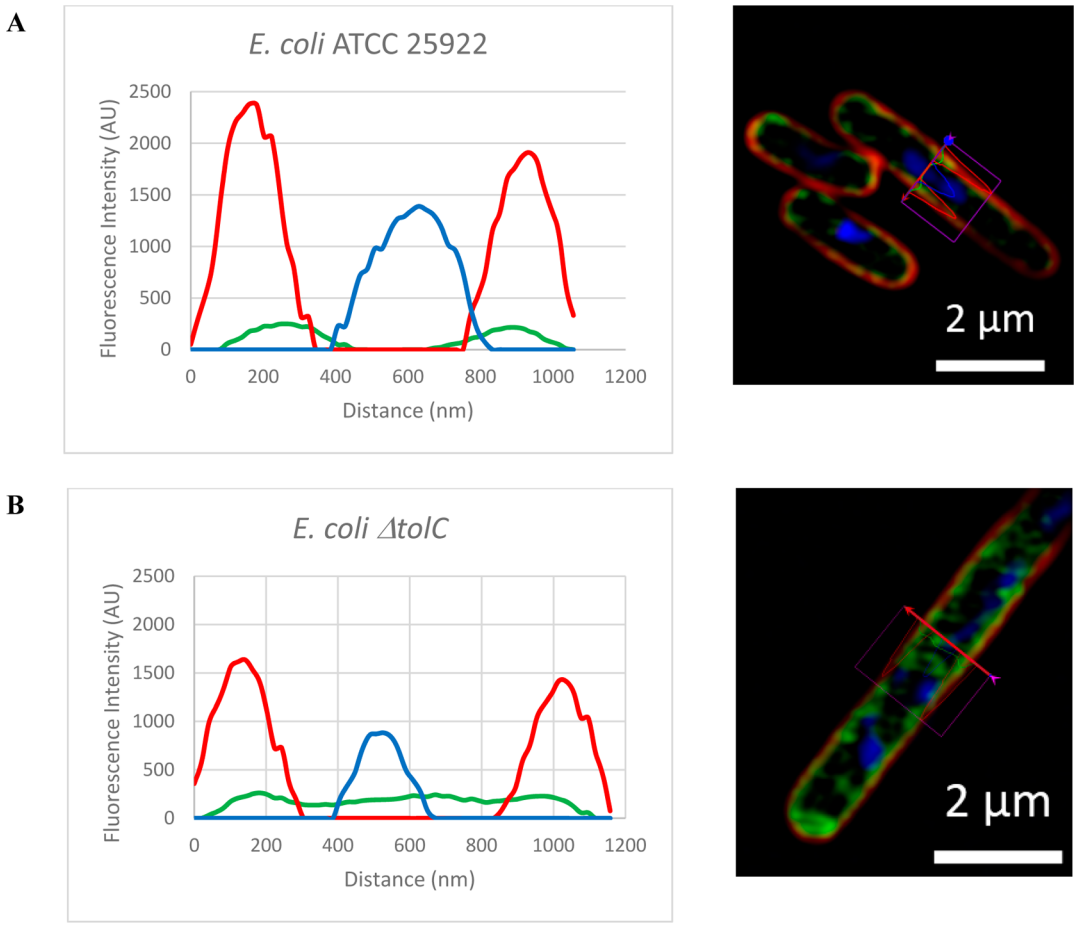

Figure 8. Cross section of fluorescent imaging of (A) *E. coli* (ATCC 25922) (B) Δ*tolC E. coli*: green, TMP-fluorophore **12b**; red, FM4-64FX (bacterial membrane stain); blue, Hoechst 33342 (nucleic acid stain). The images were processed using the "enabling raw scale" option.

of the analyte **12b** and could be used to monitor the stability of **12b** in LC-MS/MS samples. An LC-MS/MS method was developed for quantification of **12b**, with the analogue **12a** used as the MS internal standard.[54,55]

The bacteria were treated in the same way as for the fluorescence-based assay, then washed and lysed to recover **12b** from the bacteria. Wild type *E. coli* (MIC > 64 μg/mL) was treated with **12b** at 10, 50, and 100 μM, whereas the TolC-deficient (Δ*tolC*) strain (MIC = 0.25 μg/mL = 0.37 μM) was treated with **12b** only at 50 μM. The results (Figure 6) again showed that both wild type and Δ*tolC E. coli* showed higher accumulation of **12b** in CCCP-treated than in nontreated cells, with a linear concentration dependence (Figure 6A). However, the LC-MS/MS method was not able to distinguish between the accumulation of **12b** in wild type *E. coli* versus Δ*tolC E. coli* when bacteria were incubated with a constant 50 μM (Figure 6B). The results from the LC-MS/MS assay were generally consistent with the results from fluorescence-based assay, apart from this lack of discrimination between the wild type and Δ*tolC* mutant strains.

The observation that cellular accumulations were higher than extracellular concentration (ranging from 4- to 8-fold) is consistent with previous results for accumulation assay using LC-MS/MS. Active import and Donnan potential have been suggested as mechanisms that may account for this accumulation.[54,55]

Fluorescence Microscopy. Super-resolution structured illumination microscopy (SR-SIM) has been used for imaging in bacteria to overcome the resolution barrier resulting from the small size of bacterial cells, which prevents good visualization by standard confocal microscopy.[69,70] As TMP is active against both Gram-positive and Gram-negative bacteria, *Staphylococcus aureus* (ATCC 25923) and *E. coli* (ATCC 25922) were stained with TMP probe **12b**. Both showed labeling at a concentration of 100 μM versus MIC values of >64 μg/mL (94 μM) and 16 μg/mL (24 μM), respectively (Figure 7). SR-SIM fluorescent imaging with membrane (FM4-64FX) and nucleic acid (Hoechst 33342) costaining showed that the membrane dye was quickly endocytosed in *S. aureus*, even though this Gram-positive bacteria was stained with FM4-64FX for only 1 min (Figure 7A). To compare fluorescence brightness, SR-SIM images were processed using the "enabling raw scale" option. A surface plot showed the relative fluorescence brightness of each fluorescent probe (Figure 7B).

Cross sections of representative bacteria (Figure 8) clearly demonstrated that the **12b** probe was largely localized *inside* the bacterial membrane when compared to the location of the red FM4-64FX dye, but generally remained associated with the cell wall/membrane structure, possibly due to either binding to DHFR or internal components of efflux pumps. Some internal cellular staining was also evident, which was notably stronger in the Δ*tolC* mutant, and was consistent with higher cellular accumulation. Cross sections of bacteria when images were processed without enabling raw scale are shown in Figure S2. Staining with the NBD-alkyne dye **9** alone did not result in significant bacterial labeling (Figure S1). The intracellular

DOI: 10.1021/acsinfecdis.6b00080
ACS Infect. Dis. 2016, 2, 688−701

localization of DHFR has not been reported in the literature, and this study suggests that it may be associated with the internal cell wall/membrane structure, as opposed to freely distributed in the cytoplasm.

CONCLUSION

We have synthesized azide-functionalized TMP analogues that strongly inhibited the TMP enzymatic target *e*DHFR in vitro and retained moderate antibacterial activity against *E. coli* strains. Reaction of these azide-containing TMPs with alkyne-fluorophores using CuAAC generated a TMP fluorescent probe library. These probes, despite generally good *e*DHFR inhibition, lost almost all ability to inhibit wild type *E. coli* growth. Activity was restored when tested against the TolC-deficient (Δ*tolC*) strain, indicating that in normal bacteria TMP probe accumulation at a sufficiently high concentration to inhibit the DHFR target was prevented due to removal by the TolC-dependent efflux pump system.

We then used the fluorescent TMP probe **12b** to develop fluorescence-based assays to measure cellular accumulation of the probe. Notably, minimal sample manipulation was required for these fluorescence-based assays using either fluorescence spectrometry or flow cytometry. The cellular fluorescence intensity was directly measured without the need for cell lysis.

The development of alternative assays to show the roles of efflux pumps on intracellular accumulation provides important tools for antibiotic drug discovery and development. To date, fluorescent and radiometric detection methods have been used to determine intracellular drug concentration and efflux pump effects.[71,72] Fluorescence was used to measure the accumulation of quinolone class compounds,[73] but this method is only applicable to intrinsically fluorescent compounds. Radiometric detection needs radiolabeled analogues and a specific instrument for counting.[55,71] An ethidium bromide-agar cartwheel method has also been used to assess the presence of MDR efflux pumps,[74,75] but ethidium bromide is rigorously controlled in many countries.[76,77] The fluorescent probes 1-*N*-phenylnaphthylamine (NPN) and 2-(4-dimethylaminostyryl)-1-ethylpyridinium iodide (DMP) (which are weakly fluorescent in an aqueous environment but fluoresce more intensely in a nonpolar environment such as the phospholipid layer of the outer membrane in Gram-negative bacteria) have been used to determine bacterial penetration of compounds and the effect of efflux pump inhibitors.[11,78,79]

Methods based on LC-MS analysis have been developed to quantify compound accumulation in bacterial cells.[54,55,80,81] The LC-MS technique is a useful method for a wide range of structurally different compounds including unlabeled compounds, but is time-consuming as bacterial cells need to be lysed and the supernatant isolated to prepare samples for LC-MS. The development of a rapid fluorescence-based assay to assess inhibition of efflux pumps, as outlined in this study, is a potentially useful research tool in the search for new antibiotics and antibiotic adjuvants.

METHODS

For chemical synthesis please see the Supporting Information.

Minimum Inhibitory Concentration Determination. Bacteria were obtained from the American Type Culture Collection (ATCC; Manassas, VA, USA), Merck Sharp & Dohme (Kenilworth, NJ, USA), the Coli Genetic Stock Center (CGSC, Yale University), and independent academic clinical isolate collections. Bacteria were cultured in Muller−Hinton broth (MHB) (Bacto Laboratories, catalog no. 211443) at 37 °C overnight. A sample of each culture was then diluted 50-fold in MHB and incubated at 37 °C for 1.5−3 h. The compounds were serially diluted 2-fold across the wells, with concentrations ranging from 0.06 to 128 μg/mL, plated in duplicate. The resultant mid log phase cultures were diluted to the final concentration of 5×10^5 CFU/mL, and then 50 μL was added to each well of the compound-containing 96-well plates (Corning; catalog no. 3641, NBS plates), giving a final compound concentration range of 0.03−64 μg/mL. All of the plates were covered and incubated at 37 °C for 18 h with the MIC defined as the lowest compound concentration at which no bacterial growth was visible ($n = 4$).

Cytotoxicity Assay (Resazurin Assay). The compounds were provided at a stock concentration of 12 mM in 100% DMSO. A dilution series in DMEM + 10% FBS was carried out in a one in two step decrease to give the 2× concentrated range from 120 to 1.0 μM. Twenty microliters of each dilution was added to a 384-well black-wall clear-bottom tissue culture plate (Corning; catalog no. 3712) in $n = 2$. No cells served as negative control ("all cells are dead"), and in addition a serial dilution of tamoxifen (Sigma-Aldrich, catalog no. T5648), starting at 200 μM final concentration, was included as a dose response control. HEK293 and HepG2 cells were seeded into the plates containing the compounds, at 4000 and 5000 per well, respectively, in a volume of 20 μL in DMEM + 10% of FBS ($V_{total} = 40$ μL), giving the final compound concentration range from 60 to 0.5 μM. The cells together with the compounds were incubated for 20 h at 37 °C, 5% CO_2. After the incubation, 5 μL of 100 μM resazurin (Sigma-Aldrich, catalog no. R7017) dissolved in PBS was added to each well (final concentration = 11 μM). The plates were then incubated for 3 h at 37 °C, 5% CO_2. The fluorescence intensity was read using the TECAN Infinite M1000 PRO with excitation/emission 560/590 nm. The data were analyzed by GraphPad Prism 7.00 software. Results are presented as the average percentage of control ± SD for each set of duplicate wells using the following equation: cell survival % = $(FI_{sample} - FI_{negative}/FI_{untreated} - FI_{negative}) \times 100$.

DHFR Enzyme Inhibition assay. The inhibition of DHFR with TMP derivatives was investigated in a 96-well plate (flat-bottom wells, Nunclon Delta Cell Culture Treated Clear Polystyrene catalog no. 167008) using a dihydrofolate reductase assay kit (Sigma-Aldrich, product code CS0340). *E. coli* dihydrofolate reductase was prepared using an *In Vitro* protein synthesis kit (New England BioLabs; PURExpress *In Vitro* Protein Synthesis; NEB#E6800). The DHFR enzyme was diluted before using in the inhibition assay by adding 23 μL of DHFR in 1 mL of water. The assay was performed using the protocol supplied by Sigma-Aldrich; however, the procedure was adjusted for a reaction volume of 200 μL. Briefly, the compounds were provided at a stock concentration of 12 mM in 100% DMSO. The 1× buffer mixture for assay was composed of DHF and NADPH. The well containing 100 μM TMP served as negative control ("DHFR is completely inhibited") and the well without TMP or the untreated well served as positive control ("DHFR is not inhibited"). A dilution series of compounds in water was carried out to give the 3× concentrated range from 120 to 0.018 μM. Ten microliters of each dilution was added to a 96-well plate containing 180 μL of buffer mixture. Then, 10 μL of diluted DHFR was added into each well, giving the final compound concentration range from

DOI: 10.1021/acsinfecdis.6b00080
ACS Infect. Dis. 2016, 2, 688−701

6 to 0.0009 μM. The samples were immediately read by the plate reader. The reaction progress was monitored by the decrease in absorbance at 340 nm, which was read every 60 s for 40 min using a POLARstar Omega plate reader, with enzymatic inhibition calculated using the equation DHRF activity % = (Abs_{sample} − $Abs_{negative}$/$Abs_{untreated}$ − $Abs_{negative}$) × 100. The data were analyzed by GraphPad Prism 7.00 software to determine IC_{50} values.

Preparation of Bacterial Cell for Fluorescence Measurement and LC-MS/MS. Bacteria were cultured in Luria broth (LB) (AMRESCO, catalog no. J106) at 37 °C overnight. A sample of each culture was then diluted 50-fold in LB and incubated at 37 °C for 1.5−2 h. The resultant mid log phase cultures were harvested at 4000 rpm for 25 min, washed once with PBS (4000 rpm, for 15 min), and resuspended in PBS to an OD_{600} of 2. Bacteria were treated with CCCP (Sigma-Aldrich, catalog no. C2759) (100 μM, 37 °C, 10 min) in PBS and then with the TMP probe at the desired concentration (37 °C, 30 min) and washed with 1 mL of cold water four times (13000 rpm, 4 °C, 7 min). For fluorescence intensity measurement using the plate reader, the flat-bottom black opti-plate 96 F (PerkinElmer, catalog no. 6005279) was chosen for this fluorescence assay as it shows less background noise and is suitable for measurements of fluorescence intensity.[55] Bacteria cell pellets were transferred into a 96-well plate in a final volume of 150 μL in PBS. The fluorescence intensity was read using the TECAN Infinite M1000 PRO with excitation/emission at 475/545 nm. For fluorescence intensity measurement using the flow cytometer (Gallios flow cytometer from Beckman Coulter), bacteria cell pellets were resuspended in 1 mL of PBS. The sample was then read on the cytometer at a flow rate of approximately 60 μL/min, logarithmic amplification was used for the data acquisition, and the core diameter was calculated to be 6 μm. A total of 10000 events were collected, and the data were analyzed using Kaluza Analysis 1.3 software. Fluorescent intensity from FL1 (excitation, 488 nm; emission, 525/20 nm), was plotted against the number of events count. Median fluorescent intensity was estimated from the histogram peaks after the bacteria had been stained with the TMP probe.

Preparation of Bacterial Cell Extract for LC-MS/MS Analysis. Bacteria were lysed by adding 180 μL of enzymatic lysis buffer, 20 mM Tris-HCl, pH 8.0, and 2 mM sodium EDTA, followed by 70 μL of lysozyme (stock concentration = 72 mg/mL in H_2O), then incubated at 37 °C for 30 min, freeze (−78 °C, 5 min)−thawed (34 °C, 15 min) for three cycles, sonicated for 20 min, and then heated to 65 °C for 30 min. The lysate was then centrifuged (14000 rpm, 8 min), and then the supernatants were filtered through a filter membrane 10 kDa (Merck, Amicon Ultra-0.5 centrifugal filter unit with Ultracel-10 membrane catalog no. UFC501096) (14000 rpm, 5 min), which was washed four times with 100 μL of water. The filtered supernatants were lyophilized and then redissolved in 150 μL of acetonitrile/methanol/10 mM **12a** (internal control sample) in DMSO (1:1:0.0001) solution. The samples were kept at 4 °C for 1 h to precipitate impurities and centrifuged (14000 rpm, 8 min), and the supernatants were transferred to a vial for LC-MS/MS analysis.

LC-MS/MS Conditions. Sample analysis was performed using an AB Sciex 4000 QTRAP system (USA) and a Shimadzu Nexara UPLC system (Japan) using a Waters Atlantis T3 column (2.1 × 50 mm, 5 μm) with a guard column. The column oven was set at 40 °C. Mobile phases were (A) water/formic acid (1:0.001, v/v) and (B) acetonitrile/formic acid (1:0.001, v/v). The gradient started at 2% B for 1 min, then 2−100% B for 8 min. The flow rate was set to 0.2 mL/min, and the autosampler was maintained at 12 °C. Injection volumes of 5 μL per sample were injected for uptake assays using 10 μM **12b**, whereas 3 μL per sample was injected for uptake assays using 50 and 100 μM **12b**. Source/gas parameters were as follows: curtain gas (CUR) at 35, ion spray voltage (IS) at 5500, temperature (TEM) at 500, ion source gas 1 (GS1) at 50, and ion source gas 2 (GS2) at 50. Multiple reaction monitoring (MRM) transitions were monitored in the positive mode. Collision energy (CE) and declustering potential (DP) were optimized to generate a good response signal. **12a** m/z was at 578.4 → 123.1 (DP = 90 and CE = 50), and **12b** m/z was at 592.3 → 316.3 and 592.3 → 123.1 (DP = 45 and CE = 45).

Calibration curves were acquired by plotting the standard concentration against its peak area. Standard concentrations ranged from 0.01 to 6.67 μM for the uptake assay using 10 μM **12b**, and standard concentrations from 0.07 to 22.22 μM for the uptake assay using 50 and 100 μM **12b** were prepared in acetonitrile/methanol/10 mM **12a** in DMSO (50:50:0.005, v/v) solution. For each assay, the standard calibration curve was obtained by plotting the standard concentration against the response peak area in the mass spectrometer. A linear regression of at least 0.99 was then established before using the standard curve in computations.

Cellular Concentration Calculation in *E. coli*. In the LC-MS/MS assay, each sample had 2×10^9 cells using 1 μm^3 as the cellular volume of *E. coli*.[55,82] The cellular concentration was calculated on the basis of the calculation in a previous study from Cai et al.[55] Thus, the total volume of *E. coli* 2×10^9 cells is 2 μL [$(2 \times 10^9) \times 1\ \mu m^3 = 2 \times 10^9\ \mu m^3 = 2\ \mu L$ (1 mL = $1 \times 10^{12}\ \mu m^3$)]. Therefore, the cellular concentration was equal to the measured concentration using LC-MS/MS (in μM) multiplied by the extraction volume (150 μL) and divided by the total cellular volume per sample (2 μL). For example, for the measured **12b** of 7.122 μM, the cellular concentration would be 534.15 μM [(7.122 μM × 150 μL)/2 μL = 534.15 μM].

Fluorescence Microscopy; Structured Illumination Microscopy (SIM). SIM was performed using the Zeiss Elyra PS.1 SIM/STORM microscope. Images were analyzed with ZEN2012. To compare fluorescence intensity, the "raw scale" option was used to process images. VectaShield H1000 was used as a mounting medium. Coverslip glasses (Zeiss/Schott, 18 mm × 18 mm, no. 1.5H) were used to prepare samples. Hank's balanced salt solution (HBSS) without phenol red, $CaCl_2$, or $MgSO_4$ (Sigma-Aldrich catalog no. H6648) was used for bacterial staining. Fluorescent dyes FM4-64FX and Hoechst 33342 (Life Technologies, Australia) were used for membrane staining and DNA staining, respectively.

S. aureus (ATCC 25923) and *E. coli* were cultured in LB at 37 °C overnight. A sample of each culture was then diluted 50-fold in LB and incubated at 37 °C for 1.5−2 h. One milliliter of the resultant mid log phase cultures was transferred to an Eppendorf tube and centrifuged. Bacteria were washed once with HBSS and then suspended in 20 μL of HBSS. Two microliters of this suspended bacteria solution was dropped onto a coverslip, spread, and dried. Probe **12b** (200 μL, 100 μM) was then added to the bacteria, left for 30 min at room temperature, and then washed once with HBSS. An ice-cold solution (200 μL) of Hoechst 33342 (5 μg/mL in HBSS) was then dropped onto the bacteria, left for 10 min on ice, and then drained. This was followed by adding an ice-cold solution (200

DOI: 10.1021/acsinfecdis.6b00080
ACS Infect. Dis. 2016, 2, 688−701

μL) of FM4-64FX (5 μg/mL in HBSS) onto the bacteria, which was left for 5 min for *E. coli* and for 1 min for *S. aureus* on ice. The bacteria were then washed once with ice-cold HBSS. The bacteria were fixed with 4% paraformaldehyde for 20 min for *E. coli* and for 10 min for *S. aureus* on ice, followed by mounting on slides using VectaShield H1000 as a mounting medium.

■ ASSOCIATED CONTENT

Supporting Information

The Supporting Information is available free of charge on the ACS Publications website at DOI: 10.1021/acsinfecdis.6b00080.

Methods, synthesis, compound characterization, and NMR spectrum; details of *E. coli* strains; fluorescent imaging of the control probe; fluorescent imaging of **12b** without raw scale applied; excitation/emission spectra of TMP probes (PDF)

■ AUTHOR INFORMATION

Corresponding Authors

*(M.A.T.B.) E-mail: m.blaskovich@uq.edu.au. Fax: +61-7-3346-2090. Phone: +61-7-3346-2994.

*(M.A.C.) E-mail: m.cooper@uq.edu.au. Phone: +61-7-3346-2044.

Author Contributions

M.A.T.B., M.S.B., M.A.C., and W.P. conceived the study. W.P., R.P., M.S.B., S.K., M.P., and G.K. performed the experiments and analyzed the data. W.P., M.S.B., and M.A.T.B. wrote the paper with input from all authors.

Notes

The authors declare no competing financial interest.

■ ACKNOWLEDGMENTS

M.A.C. is supported by a NHMRC Principal Research Fellowship (APP1059354), W.P. and S.K. are supported by a UQ International Scholarship (UQI) and IMB Postgraduate Award (IMBPA), and M.P. is supported by an Australian Postgraduate Award (APA) Ph.D. scholarship. R.P., M.A.T.B., M.S.B., and G.K. are supported in part by Wellcome Trust Strategic Grant WT141107. Imaging work was performed in the Queensland Brain Institute's Advanced Microscopy Facility and generously supported by ARC LIEF LE130100078. We thank Luke Alexander Hammond for training and data analysis. The wild type and mutant *tolC* and *lpxC* and double-mutant *E. coli* strains MB4827, MB4902, MB5746, and MB5747 were generously supplied by Merck Sharp & Dohme (Kenilworth, NJ, USA).

■ REFERENCES

(1) Xu, Z.-Q., Flavin, M. T., and Flavin, J. (2014) Combating multidrug-resistant Gram-negative bacterial infections. *Expert Opin. Invest. Drugs 23*, 163−182.

(2) Cloete, T. E. (2003) Resistance mechanisms of bacteria to antimicrobial compounds. *Int. Biodeterior. Biodegrad. 51*, 277−282.

(3) Vranakis, I., Goniotakis, I., Psaroulaki, A., Sandalakis, V., Tselentis, Y., Gevaert, K., and Tsiotis, G. (2014) Proteome studies of bacterial antibiotic resistance mechanisms. *J. Proteomics 97*, 88−99.

(4) Blair, J. M. A., Webber, M. A., Baylay, A. J., Ogbolu, D. O., and Piddock, L. J. V. (2015) Molecular mechanisms of antibiotic resistance. *Nat. Rev. Microbiol. 13*, 42−51.

(5) Amaral, L., Martins, A., Spengler, G., and Molnar, J. (2014) Efflux pumps of Gram-negative bacteria: what they do, how they do it, with what and how to deal with them. *Front. Pharmacol. 4*, 1−11.

(6) Poole, K. (2012) Efflux-mediated antimicrobial resistance. In *Antibiotic Discovery and Development* (Dougherty, T. J., and Pucci, M. J., Eds.), 1st ed., pp 349−395, Springer, New York.

(7) Chollet, R., Chevalier, J., Bryskier, A., and Pagès, J.-M. (2004) The AcrAB-Tolc pump is involved in macrolide resistance but not in telithromycin efflux in *Enterobacter aerogenes* and *Escherichia coli*. *Antimicrob. Agents Chemother. 48*, 3621−3624.

(8) Piddock, L. J. V. (2006) Clinically relevant chromosomally encoded multidrug resistance efflux pumps in bacteria. *Clin. Microbiol. Rev. 19*, 382−402.

(9) Nichols, W. W. (2012) Permeability of bacteria to antibacterial agents. In *Antibiotic Discovery and Development* (Dougherty, T. J., and Pucci, M. J., Eds.), 1st ed., pp 849−879, Springer: New York.

(10) Wang, Y., Venter, H., and Ma, S. (2016) Efflux pump inhibitors: a novel approach to combat efflux-mediated drug resistance in bacteria. *Curr. Drug Targets 17*, 702−719.

(11) Lomovskaya, O., Warren, M. S., Lee, A., Galazzo, J., Fronko, R., Lee, M., Blais, J., Cho, D., Chamberland, S., Renau, T., Leger, R., Hecker, S., Watkins, W., Hoshino, K., Ishida, H., and Lee, V. J. (2001) Identification and characterization of inhibitors of multidrug resistance efflux pumps in *Pseudomonas aeruginosa*: novel agents for combination therapy. *Antimicrob. Agents Chemother. 45*, 105−116.

(12) Li, X.-Z., and Nikaido, H. (2004) Efflux-mediated drug resistance in bacteria. *Drugs 64*, 159−204.

(13) Sun, J., Deng, Z., and Yan, A. (2014) Bacterial multidrug efflux pumps: mechanisms, physiology and pharmacological exploitations. *Biochem. Biophys. Res. Commun. 453*, 254−267.

(14) Jamshidi, S., Sutton, J. M., and Rahman, K. M. (2016) An overview of bacterial efflux pumps and computational approaches to study efflux pump inhibitors. *Future Med. Chem. 8*, 195−210.

(15) Bakshi, S., Siryaporn, A., Goulian, M., and Weisshaar, J. C. (2012) Superresolution imaging of ribosomes and RNA polymerase in live *Escherichia coli* cells. *Mol. Microbiol. 85*, 21−38.

(16) Fleurie, A., Lesterlin, C., Manuse, S., Zhao, C., Cluzel, C., Lavergne, J.-P., Franz-Wachtel, M., Macek, B., Combet, C., Kuru, E., VanNieuwenhze, M. S., Brun, Y. V., Sherratt, D., and Grangeasse, C. (2014) MapZ marks the division sites and positions FtsZ rings in *Streptococcus pneumoniae*. *Nature 516*, 259−262.

(17) Strauss, M. P., Liew, A. T. F., Turnbull, L., Whitchurch, C. B., Monahan, L. G., and Harry, E. J. (2012) 3D-SIM super resolution microscopy reveals a bead-like arrangement for FtsZ and the division machinery: implications for triggering cytokinesis. *PLoS Biol. 10*, e1001389.

(18) Daniel, R. A., and Errington, J. (2003) Control of cell morphogenesis in bacteria: two distinct ways to make a rod-shaped cell. *Cell 113*, 767−776.

(19) Tiyanont, K., Doan, T., Lazarus, M. B., Fang, X., Rudner, D. Z., and Walker, S. (2006) Imaging peptidoglycan biosynthesis in *Bacillus subtilis* with fluorescent antibiotics. *Proc. Natl. Acad. Sci. U. S. A. 103*, 11033−11038.

(20) Kocaoglu, O., Calvo, R. A., Sham, L.-T., Cozy, L. M., Lanning, B. R., Francis, S., Winkler, M. E., Kearns, D. B., and Carlson, E. E. (2012) Selective penicillin-binding protein imaging probes reveal substructure in bacterial cell division. *ACS Chem. Biol. 7*, 1746−1753.

(21) Fei, X., and Gu, Y. (2009) Progress in modifications and applications of fluorescent dye probe. *Prog. Nat. Sci. 19*, 1−7.

(22) Saffarian, S., Li, Y., Elson, E. L., and Pike, L. J. (2007) Oligomerization of the EGF receptor investigated by live cell fluorescence intensity distribution analysis. *Biophys. J. 93*, 1021−1031.

(23) Holm, C., and Jespersen, L. (2003) A flow-cytometric Gram-staining technique for milk-associated bacteria. *Appl. Environ. Microbiol. 69*, 2857−2863.

(24) Thurn, K. T., Paunesku, T., Wu, A., Brown, E. M. B., Lai, B., Vogt, S., Maser, J., Aslam, M., Dravid, V., Bergan, R., and Woloschak, G. E. (2009) Labeling TiO_2 nanoparticles with dyes for optical

DOI: 10.1021/acsinfecdis.6b00080
ACS Infect. Dis. 2016, 2, 688−701

fluorescence microscopy and determination of TiO_2−DNA nanoconjugate stability. *Small 5*, 1318−1325.
(25) van Oosten, M., Schäfer, T., Gazendam, J. A. C., Ohlsen, K., Tsompanidou, E., de Goffau, M. C., Harmsen, H. J. M., Crane, L. M. A., Lim, E., Francis, K. P., Cheung, L., Olive, M., Ntziachristos, V., van Dijl, J. M., and van Dam, G. M. (2013) Real-time *in vivo* imaging of invasive- and biomaterial-associated bacterial infections using fluorescently labelled vancomycin. *Nat. Commun. 4*, 2584.
(26) Kolb, H. C., and Sharpless, K. B. (2003) The growing impact of click chemistry on drug discovery. *Drug Discovery Today 8*, 1128−1137.
(27) Prescher, J. A., and Bertozzi, C. R. (2005) Chemistry in living systems. *Nat. Chem. Biol. 1*, 13−21.
(28) Tron, G. C., Pirali, T., Billington, R. A., Canonico, P. L., Sorba, G., and Genazzani, A. A. (2008) Click chemistry reactions in medicinal chemistry: applications of the 1,3-dipolar cycloaddition between azides and alkynes. *Med. Res. Rev. 28*, 278−308.
(29) Yoon, H. I., Yhee, J. Y., Na, J. H., Lee, S., Lee, H., Kang, S.-W., Chang, H., Ryu, J. H., Lee, S., Kwon, I. C., Cho, Y. W., and Kim, K. (2016) Bioorthogonal copper free click chemistry for labeling and tracking of chondrocytes *in vivo*. *Bioconjugate Chem. 27*, 927−936.
(30) Avvakumova, S., Colombo, M., Tortora, P., and Prosperi, D. (2014) Biotechnological approaches toward nanoparticle biofunctionalization. *Trends Biotechnol. 32*, 11−20.
(31) Yamagishi, K., Sawaki, K., Murata, A., and Takeoka, S. (2015) A Cu-free clickable fluorescent probe for intracellular targeting of small biomolecules. *Chem. Commun. 51*, 7879−7882.
(32) Johansson, L. B. G., Simon, R., Bergström, G., Eriksson, M., Prokop, S., Mandenius, C.-F., Heppner, F. L., Åslund, A. K. O., and Nilsson, K. P. R. (2015) An azide functionalized oligothiophene ligand − a versatile tool for multimodal detection of disease associated protein aggregates. *Biosens. Bioelectron. 63*, 204−211.
(33) Phetsang, W., Blaskovich, M. A. T., Butler, M. S., Huang, J. X., Zuegg, J., Mamidyala, S. K., Ramu, S., Kavanagh, A. M., and Cooper, M. A. (2014) An azido-oxazolidinone antibiotic for live bacterial cell imaging and generation of antibiotic variants. *Bioorg. Med. Chem. 22*, 4490−4498.
(34) Eliopoulos, G. M., and Huovinen, P. (2001) Resistance to trimethoprim-sulfamethoxazole. *Clin. Infect. Dis. 32*, 1608−1614.
(35) Cassir, N., Rolain, J.-M., and Brouqui, P. (2014) A new strategy to fight antimicrobial resistance: the revival of old antibiotics. *Front. Microbiol. 5*, 551.
(36) Wang, T. Y., Friedman, Larry, J., Gelles, J., Min, W., Hoskins, A. A., and Cornish, V. W. (2014) The covalent trimethoprim chemical tag facilitates single molecule imaging with organic fluorophores. *Biophys. J. 106*, 272−278.
(37) Rajapakse, H. E., and Miller, L. W. (2012) Time-resolved luminescence resonance energy transfer imaging of protein−protein interactions in living cells. In *Methods in Enzymology* (Conn, P. M., Ed.), 1st ed., pp 329−345, Academic Press, San Diego, CA, USA.
(38) Chen, Z., Jing, C., Gallagher, S. S., Sheetz, M. P., and Cornish, V. W. (2012) Second-generation covalent TMP-tag for live cell imaging. *J. Am. Chem. Soc. 134*, 13692−13699.
(39) Wombacher, R., Heidbreder, M., van de Linde, S., Sheetz, M. P., Heilemann, M., Cornish, V. W., and Sauer, M. (2010) Live-cell super-resolution imaging with trimethoprim conjugates. *Nat. Methods 7*, 717−719.
(40) Gallagher, S. S., Jing, C., Peterka, D. S., Konate, M., Wombacher, R., Kaufman, L. J., Yuste, R., and Cornish, V. W. (2010) A trimethoprim-based chemical tag for live cell two-photon imaging. *ChemBioChem 11*, 782−784.
(41) Gallagher, S. S., Sable, J. E., Sheetz, M. P., and Cornish, V. W. (2009) An *in vivo* covalent TMP-tag based on proximity-induced reactivity. *ACS Chem. Biol. 4*, 547−556.
(42) Miller, L. W., Cai, Y., Sheetz, M. P., and Cornish, V. W. (2005) *In vivo* protein labeling with trimethoprim conjugates: a flexible chemical tag. *Nat. Methods 2*, 255−257.
(43) Jing, C., and Cornish, V. W. (2013) Design, synthesis, and application of the trimethoprim-based chemical tag for live cell imaging. *Curr. Protoc. Chem. Biol. 5*, 131−155.
(44) Karoli, T., Mamidyala, S. K., Zuegg, J., Fry, S. R., Tee, E. H. L., Bradford, T. A., Madala, P. K., Huang, J. X., Ramu, S., Butler, M. S., and Cooper, M. A. (2012) Structure aided design of chimeric antibiotics. *Bioorg. Med. Chem. Lett. 22*, 2428−2433.
(45) Yuthavong, Y. (2002) Basis for antifolate action and resistance in malaria. *Microbes Infect. 4*, 175−182.
(46) Sirichaiwat, C., Intaraudom, C., Kamchonwongpaisan, S., Vanichtanankul, J., Thebtaranonth, Y., and Yuthavong, Y. (2004) Target guided synthesis of 5-benzyl-2,4-diamonopyrimidines: their antimalarial activities and binding affinities to wild type and mutant dihydrofolate reductases from *Plasmodium falciparum*. *J. Med. Chem. 47*, 345−354.
(47) Salvatore, R. N., Yoon, C. H., and Jung, K. W. (2001) Synthesis of secondary amines. *Tetrahedron 57*, 7785−7811.
(48) Pak, Y. L., Swamy, K. M. K., and Yoon, J. (2015) Recent progress in fluorescent imaging probes. *Sensors 15*, 24374−24396.
(49) Ji, Y.-F., Jiang, J.-A., Liu, H.-W., Liao, D.-H., and Wei, X.-Y. (2013) Practical preparation of trimethoprim: a classical antibacterial agent. *Synth. Commun. 43*, 1517−1522.
(50) Fletcher, J. I., Haber, M., Henderson, M. J., and Norris, M. D. (2010) ABC transporters in cancer: more than just drug efflux pumps. *Nat. Rev. Cancer 10*, 147−156.
(51) Nishino, K., and Yamaguchi, A. (2001) Analysis of a complete library of putative drug transporter genes in *Escherichia coli*. *J. Bacteriol. 183*, 5803−5812.
(52) Marquez, B. (2005) Bacterial efflux systems and efflux pumps inhibitors. *Biochimie 87*, 1137−1147.
(53) Ghoul, M., Pommepuy, M., Moillo-Batt, A., and Cormier, M. (1989) Effect of carbonyl cyanide *m*-chlorophenylhydrazone on *Escherichia coli* halotolerance. *Appl. Environ. Microbiol. 55*, 1040−1043.
(54) Davis, T. D., Gerry, C. J., and Tan, D. S. (2014) General platform for systematic quantitative evaluation of small-molecule permeability in bacteria. *ACS Chem. Biol. 9*, 2535−2544.
(55) Cai, H., Rose, K., Liang, L.-H., Dunham, S., and Stover, C. (2009) Development of a liquid chromatography/mass spectrometry-based drug accumulation assay in *Pseudomonas aeruginosa*. *Anal. Biochem. 385*, 321−325.
(56) Tamber, S., and Hancock, R. E. W. (2003) On the mechanism of solute uptake in *Pseudomonas*. *Front. Biosci., Landmark Ed. 8*, 472−483.
(57) Galdiero, S., Falanga, A., Cantisani, M., Tarallo, R., Pepa, M. E. D., D'Oriano, V., and Galdiero, M. (2012) Microbe-host interactions: structure and role of Gram-negative bacterial porins. *Curr. Protein Pept. Sci. 13*, 843−854.
(58) Anes, J., McCusker, M. P., Fanning, S., and Martins, M. (2015) The ins and outs of RND efflux pumps in *Escherichia coli*. *Front. Microbiol. 6*, 587.
(59) Zgurskaya, H. I. (2009) Multicomponent drug efflux complexes: architecture and mechanism of assembly. *Future Microbiol. 4*, 919−932.
(60) Mason, D. J., Shanmuganathan, S., Mortimer, F. C., and Gant, V. A. (1998) A fluorescent gram stain for flow cytometry and epifluorescence microscopy. *Appl. Environ. Microbiol. 64*, 2681−2685.
(61) Roth, B. L., Poot, M., Yue, S. T., and Millard, P. J. (1997) Bacterial viability and antibiotic susceptibility testing with SYTOX green nucleic acid stain. *Appl. Environ. Microbiol. 63*, 2421−2431.
(62) Ambriz-Aviña, V., Contreras-Garduño, J. A., and Pedraza-Reyes, M. (2014) Applications of flow cytometry to characterize bacterial physiological responses. *BioMed Res. Int. 2014*, 1−14.
(63) Fura, J. M., Pidgeon, S. E., Birabaharan, M., and Pires, M. M. (2016) Dipeptide-based metabolic labeling of bacterial cells for endogenous antibody recruitment. *ACS Infect. Dis. 2*, 302−309.
(64) Piddock, L. J. V., and Johnson, M. M. (2002) Accumulation of 10 fluoroquinolones by wild-type or efflux mutant *Streptococcus pneumoniae*. *Antimicrob. Agents Chemother. 46*, 813−820.
(65) Sedov, S. A., Belogurova, N. G., Shipovskov, S., Levashov, A. V., and Levashov, P. A. (2011) Lysis of *Escherichia coli* cells by lysozyme:

DOI: 10.1021/acsinfecdis.6b00080
ACS Infect. Dis. 2016, 2, 688−701

discrimination between adsorption and enzyme action. *Colloids Surf., B 88*, 131−133.
(66) Chan, K. C., Ho, S., Law, J., and Yuen, V. (2002) Microwave treatment as a substitute for EDTA in lysozyme-mediated bacterial cell lysis and its effects on bacterial protein release and β-galactosidase activity. *J. Exp. Microbiol. Immunol. 2*, 144−156.
(67) Wang, G., Lo, L. F., Forsberg, L. S., and Maier, R. J. (2013) *Helicobacter pylori* peptidoglycan modifications confer lysozyme resistance and contribute to survival in the host. *mBio 3*, e00409−e00412.
(68) Yeung, Y.-G., and Stanley, E. R. (2010) Rapid detergent removal from peptide samples with ethyl acetate for mass spectrometry analysis. *Curr. Protoc. Protein Sci. 59*, 16.12.1−16.12.5.
(69) Coltharp, C., and Xiao, J. (2012) Superresolution microscopy for microbiology. *Cell. Microbiol. 14*, 1808−1818.
(70) Turnbull, L., Strauss, M. P., Liew, A. T. F., Monahan, L. G., Whitchurch, C. B., and Harry, E. J. (2014) Super-resolution imaging of the cytokinetic Z ring in live bacteria using fast 3D-structured illumination microscopy (f3D-SIM). *J. Visualized Exp. 91*, 51469.
(71) Li, X. Z., Nikaido, H., and Poole, K. (1995) Role of mexA-mexB-oprM in antibiotic efflux in *Pseudomonas aeruginosa*. *Antimicrob. Agents Chemother. 39*, 1948−1953.
(72) Li, X.-Z., Zhang, L., and Nikaido, H. (2004) Efflux pump-mediated intrinsic drug resistance in *Mycobacterium smegmatis*. *Antimicrob. Agents Chemother. 48*, 2415−2423.
(73) Ricci, V., and Piddock, L. (2003) Accumulation of garenoxacin by *Bacteroides fragilis* compared with that of five fluoroquinolones. *J. Antimicrob. Chemother. 52*, 605−609.
(74) Martins, M., McCusker, M. P., Viveiros, M., Couto, I., Fanning, S., Pagès, J.-M., and Amaral, L. (2013) A simple method for assessment of MDR bacteria for over-expressed efflux pumps. *Open Microbiol. J. 7*, 72−82.
(75) Martins, M., Viveiros, M., Couto, I., Costa, S. S., Pacheco, T., Fanning, S., Pagès, J.-M., and Amaral, L. (2011) Identification of efflux pump-mediated multidrug-resistant bacteria by the ethidium bromide-agar cartwheel method. *In Vivo 25*, 171−178.
(76) Martins, A., and Amaral, L. (2012) Screening for efflux pump systems of bacteria by the new acridine orange agar method. *In Vivo 26*, 203−206.
(77) Paixão, L., Rodrigues, L., Couto, I., Martins, M., Fernandes, P., de Carvalho, C. C. C. R., Monteiro, G. A., Sansonetty, F., Amaral, L., and Viveiros, M. (2009) Fluorometric determination of ethidium bromide efflux kinetics in *Escherichia coli*. *J. Biol. Eng. 3*, 18−18.
(78) Helander, I. M., and Mattila-Sandholm, T. (2000) Fluorometric assessment of Gram-negative bacterial permeabilization. *J. Appl. Microbiol. 88*, 213−219.
(79) Germ, M., Yoshihara, E., Yoneyama, H., and Nakae, T. (1999) Interplay between the efflux pump and the outer membrane permeability barrier in fluorescent dye accumulation in *Pseudomonas aeruginosa*. *Biochem. Biophys. Res. Commun. 261*, 452−455.
(80) Zhou, Y., Joubran, C., Miller-Vedam, L., Isabella, V., Nayar, A., Tentarelli, S., and Miller, A. (2015) Thinking outside the "bug": a unique assay to measure intracellular drug penetration in Gram-negative bacteria. *Anal. Chem. 87*, 3579−3584.
(81) Bhat, J., Narayan, A., Venkatraman, J., and Chatterji, M. (2013) LC−MS based assay to measure intracellular compound levels in *Mycobacterium smegmatis*: linking compound levels to cellular potency. *J. Microbiol. Methods 94*, 152−158.
(82) Smither, R. (1975) Use of a coulter counter to detect discrete changes in cell numbers and volume during growth of *Escherichia coli*. *J. Appl. Bacteriol. 39*, 157−165.

DOI: 10.1021/acsinfecdis.6b00080
ACS Infect. Dis. 2016, 2, 688−701